Available online at www.sciencedirect.com
ScienceDirect
Journal of Power Sources 174 (2007) 813–817
JOURNAL OF POWER SOURCES
www.elsevier.com/locate/jpowsour

Short communication

An application of lithium cobalt nickel manganese oxide to high-power and high-energy density lithium-ion batteries

Hiroshi Yoshizawa [a,b], Tsutomu Ohzuku [b,*]

[a] *Technology Development Center, Matsushita Battery Industrial Co. Ltd., 1-1 Matsushita-cho, Moriguchi City, Osaka 570-8511, Japan*
[b] *Department of Applied Chemistry, Graduate School of Engineering, Osaka City University (OCU), Sugimoto 3-3-138, Sumiyoshi, Osaka 558-8585, Japan*

Available online 28 June 2007

Abstract

Evolved gas analysis (EGA) by mass spectroscopy (MS) was carried out for the pyrolysis of $Li_{1-x}Co_{1/3}Ni_{1/3}Mn_{1/3}O_2$ (185 mAh g^{-1} of charge capacity) and the results were compared with that of $Li_{1-x}CoO_2$ (140 mAh g^{-1}). Electrochemically prepared $Li_{1-x}Co_{1/3}Ni_{1/3}Mn_{1/3}O_2$ clearly shows that O_2 evolution begins at much higher temperature than $Li_{1-x}CoO_2$, suggesting that $Li_{1-x}Co_{1/3}Ni_{1/3}Mn_{1/3}O_2$ is superior to $LiCoO_2$ with respect to thermal stability. High-temperature XRD measurements of charged $LiCo_{1/3}Ni_{1/3}Mn_{1/3}O_2$-electrodes at 4.45 V were also carried out and shown that the decomposition product by heating was identified as a cubic spinel consisting of cobalt, nickel, and manganese. This indicates that phase change from a layered to spinel-framework structure plays a crucial role in the suppression of oxygen evolution from the solid matrix. In order to show practicability of the new material, lithium-ion batteries with graphite-negative electrodes are fabricated and examined in the R18650-hardware. The new lithium-ion batteries show high rate discharge performances, excellent cycle life, and safety together with high-energy density.
© 2007 Elsevier B.V. All rights reserved.

Keywords: Lithium cobalt nickel manganese oxide; EGA; Lithium-ion batteries

1. Introduction

During the past 15 years, increasing demands towards the high-energy density batteries stimulate material research on lithium insertion materials [1–3]. Fig. 1 shows record on energy density of R18650 (18 mm of diameter, 65.0 mm of height) developed at Matsushita Battery Industrial Co. Ltd., Japan. Lithium-ion batteries consisting of $LiCoO_2$ and graphite approach 500 Wh dm^{-3} in volumetric energy density in 2002, *i.e.,* HG1.8Ah, A2.0Ah, and C2.2Ah. The volumetric energy density of 500 Wh dm^{-3} is one of the critical values on $LiCoO_2$ with graphite when we provide the batteries commercially with high-rate capability and long cycle life together with safety even in an abused use. In order to cope with a critical value of 500 Wh dm^{-3}, positive-electrode material of $LiCoO_2$ has been improved by doping magnesium or another element in $LiCoO_2$ [4], resulting in energy densities more than 500 Wh dm^{-3} for high-energy density type R18650, *i.e.*, D2.4Ah and E2.6Ah for the high-energy type and CC2.0Ah for a high-power type in Fig. 1. However, high-energy and high-power type lithium-ion batteries are hard to design unless material innovation can be done.

Lithium nickel manganese oxides with or without cobalt have been investigated as possible alternatives to $LiCoO_2$ during the past 6 years in our research group [5–11]. In previous papers [12,13], we have reported the cell performance on prismatic lithium-ion batteries of $LiCo_{1/3}Ni_{1/3}Mn_{1/3}O_2$ with graphite together with some results on safety inspection by DSC and ARC. For high-power applications of lithium-ion batteries, such as hybrid electric vehicles or power tools, thermal behaviors associated with thermal runway [14,15] are extremely important in evaluating electrode materials in addition to electrochemical performance and materials economy. In this paper, we report the thermal behaviors of electrochemically charged $LiCo_{1/3}Ni_{1/3}Mn_{1/3}O_2$ and discuss whether or not the lithium insertion material of lithium cobalt nickel manganese oxide is a suitable positive-electrode material for such practical applications.

* Corresponding author.
E-mail address: ohzuku@a-chem.eng.osaka-cu.ac.jp (T. Ohzuku).

0378-7753/$ – see front matter © 2007 Elsevier B.V. All rights reserved.
doi:10.1016/j.jpowsour.2007.06.153

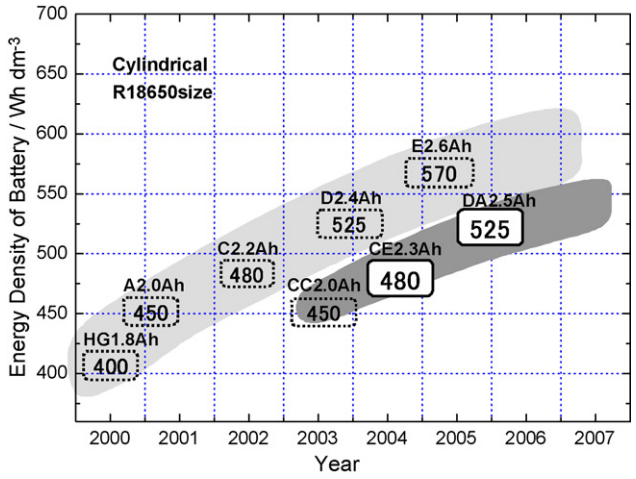

Fig. 1. Record on volumetric energy density of cylindrical lithium-ion batteries (R18650) developed at Matsushita Battery Industrial Co. Ltd., Japan. Upper group indicates high-energy density type and lower group indicates high-power type. Lithium-ion batteries called HG1.8Ah, A2.0Ah, and C2.2Ah consist of $LiCoO_2$ and graphite. Batteries called CC2.0Ah, D2.4Ah, and E2.6Ah consist of improved $LiCoO_2$ and graphite. New batteries called CE2.3Ah and DA2.5Ah are designed for high-energy and high-power applications (see in text).

2. Experimental

Methods to prepare $LiCo_{1/3}Ni_{1/3}Mn_{1/3}O_2$, electrodes, or cells are the same as described in a previous paper [12]. The prepared sample was characterized by XRD (X'Pert, Philips) and BET surface area. Morphology of particles was observed by scanning electron microscope (S-4500 Hitachi Co. Ltd., Japan). Evolved gas analysis by mass spectroscopy (EGA/MS) was performed using Agilent Technologies 6890N GC and MS-5973N MS combined with pyrolyzer (PY-2020iD, FFRONTIER LAB). Helium was used as a carrier gas at a flow rate of 1 $cm^3\,min^{-1}$. About 5 mg of the samples was precisely weighted and put in the chamber of pyrolyzer. Pyrolysis temperature was scanned from 40 °C to 700 °C at a rate of 10 °C min^{-1} and then kept at 700 °C for 14 min. Generated gas by pyrolysis was introduced into MS via a tube column maintained at 300 °C. Thermal stability tests on positive electrodes, so-called hot-pot tests, were also performed to examine whether or not thermal decomposition of electrode materials releasing oxygen relates to the thermal runaway. For the tests, the positive electrodes were taken out from charged cells and heated in the enclosed cylindrical can made of nickel-plated steel to 300 °C at a rate of 5 °C min^{-1}. Other sets of experimental conditions are given in the following Section.

3. Results and discussion

Prepared sample of $LiCo_{1/3}Ni_{1/3}Mn_{1/3}O_2$ was characterized by XRD. Crystal structure was identified as a layered structure ($a = 2.864$ Å and $c = 14.243$ Å in hexagonal setting). The calculated density was 4.75 g cm^{-3}. Morphology of particles observed by SEM is shown in Fig. 2. An average diameter of secondary particles is about 10 μm with small primary particles less than 1 μm in diameter. Particles crystallize well and nonporous body with smooth crystal surface is seen in

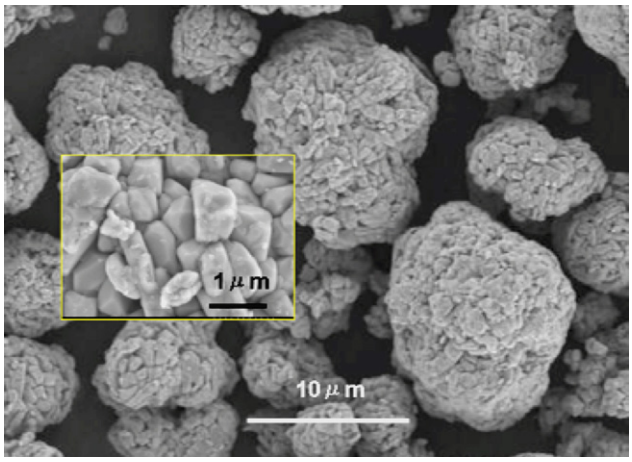

Fig. 2. Particle morphology of $LiCo_{1/3}Ni_{1/3}Mn_{1/3}O_2$ observed by SEM.

Fig. 2. BET surface area is 0.40 $m^2\,g^{-1}$. These characters of the particles are not significantly different from current $LiCoO_2$. Fig. 3(a) shows the charge and discharge curves of a Li/$LiCo_{1/3}Ni_{1/3}Mn_{1/3}O_2$ cell operated at a rate of 0.26 mA cm^{-2} in voltage of 3.0–4.45 V at 20 °C. The electrolyte used is 1.25 M $LiPF_6$ dissolved in ethylene carbonate (EC)/ethyl methyl carbonate (EMC) (1/3 by volume). The charge and discharge curves of a Li/$LiCoO_2$ cell are also shown in Fig. 3(b). The cell was operated at 0.26 mA cm^{-2} in voltage of 3.0–4.2 V. As seen in Fig. 3, $LiCo_{1/3}Ni_{1/3}Mn_{1/3}O_2$ shows rechargeable capacity of 173 mAh g^{-1} with an average voltage of 3.85 V while $LiCoO_2$ shows rechargeable capacity of 142 mAh g^{-1} with an average voltage of about 3.9 V.

Fig. 4 shows the results on so-called hot-pot tests for electrochemically charged $LiCo_{1/3}Ni_{1/3}Mn_{1/3}O_2$- and $LiCoO_2$-positive electrodes. In order to prepare the samples for hot-pot tests, $LiCo_{1/3}Ni_{1/3}Mn_{1/3}O_2$ or $LiCoO_2$ electrode was charged in lithium-ion batteries with graphite-negative electrode. Onset temperature at which temperature on sample holder deviates from that in an oven due to heat generation from the charged

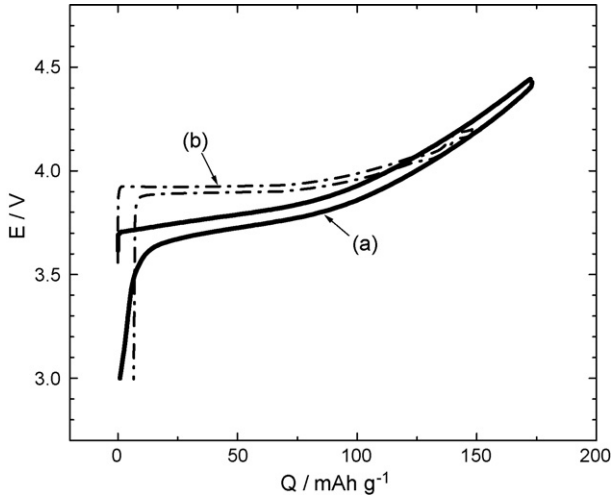

Fig. 3. Charge and discharge curves of (a) Li/$LiCo_{1/3}Ni_{1/3}Mn_{1/3}O_2$ and (b) Li/$LiCoO_2$ cells operated in voltages of 3.0–4.45 V and 3.0–4.2 V, respectively, at 20 °C.

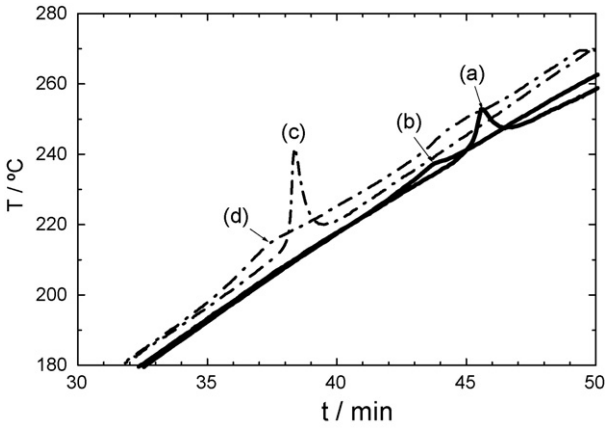

Fig. 4. Results on so-called hot-pot tests for charged $LiCo_{1/3}Ni_{1/3}Mn_{1/3}O_2$- and $LiCoO_2$-positive electrodes prepared at several charge-end voltages in lithium-ion batteries with graphite-negative electrode: (a) $Li_{1-x}Co_{1/3}Ni_{1/3}Mn_{1/3}O_2$ charged at 4.4 V, (b) $Li_{1-x}Co_{1/3}Ni_{1/3}Mn_{1/3}O_2$ charged at 4.7 V, (c) $Li_{1-x}CoO_2$ charged at 4.2 V, and (d) $Li_{1-x}CoO_2$ charged at 4.7 V.

$LiCo_{1/3}Ni_{1/3}Mn_{1/3}O_2$ at 4.4 V is about 230 °C. Onset temperature shifts to lower temperature when the sample is prepared at high voltage of 4.7 V. Onset temperature for charged $LiCoO_2$ at 4.2 V in lithium-ion batteries is about 210 °C, which is *ca.* 20 °C lower temperature than that for $LiCo_{1/3}Ni_{1/3}Mn_{1/3}O_2$. In other words, $LiCo_{1/3}Ni_{1/3}Mn_{1/3}O_2$ is thermally more stable than $LiCoO_2$ when we compare thermal behavior of highly charged state of $LiCo_{1/3}Ni_{1/3}Mn_{1/3}O_2$ at 4.4 V *(ca.* 175 mAh g^{-1} of charge capacity) with that of $LiCoO_2$ at 4.2 V (*ca.* 150 mAh g^{-1}).

Fig. 5 shows the EGA/MS results on charged $LiCo_{1/3}Ni_{1/3}Mn_{1/3}O_2$ (185 mAh g^{-1} of charge capacity) and $LiCoO_2$ (140 mAh g^{-1}). To examine intrinsic thermal behaviors of these materials, $Li_{1-x}Co_{1/3}Ni_{1/3}Mn_{1/3}O_2$ and $Li_{1-x}CoO_2$ were prepared by the electrochemical oxidation in lithium non-aqueous cells operated at 8 mA g^{-1} with no carbon and organic binder. The cells used are 2016-coin hardware. The MS signals of 31.7–32.7 in *m/z* corresponding to O_2 are illustrated in Fig. 5. Charged samples were washed with EMC and dried in vacuum before EGA/MS analysis. Oxygen is detected at temperature below 200 °C and two humps at *ca.* 240 and 280 °C are observed for $Li_{1-x}CoO_2$ (140 mAh g^{-1}). Two humps are also observed for $Li_{1-x}Co_{1/3}Ni_{1/3}Mn_{1/3}O_2$ (185 mAh g^{-1}). Their temperatures are *ca.* 260 °C and 480 °C, which are higher temperatures than those observed for $Li_{1-x}CoO_2$ (140 mAh g^{-1}). As can be clearly seen in Fig. 5, oxygen gas evolution from $Li_{1-x}Co_{1/3}Ni_{1/3}Mn_{1/3}O_2$ by heating is suppressed remarkably compared with that from $Li_{1-x}CoO_2$ in spite of highly charged state of $Li_{1-x}Co_{1/3}Ni_{1/3}Mn_{1/3}O_2$, indicating that $LiCo_{1/3}Ni_{1/3}Mn_{1/3}O_2$ is higher thermal stability than $LiCoO_2$.

In order to identify the decomposition product of charged $LiCo_{1/3}Ni_{1/3}Mn_{1/3}O_2$ electrode, high-temperature XRD measurements were carried out. Fig. 6 shows XRD patterns of decomposition products obtained by heating the charged $LiCo_{1/3}Ni_{1/3}Mn_{1/3}O_2$-electrode at 400 °C. $Li_{1-x}Co_{1/3}Ni_{1/3}Mn_{1/3}O_2$ was prepared by charging lithium cells of $LiCo_{1/3}Ni_{1/3}Mn_{1/3}O_2$ at a rate of 0.26 mA cm^{-2} to charge-end voltage of 4.45 V. Decomposition product of cobalt nickel manganese hydroxide, used to prepare $LiCo_{1/3}Ni_{1/3}Mn_{1/3}O_2$, by heating at 600 °C is also shown in Fig. 6, which is identified as cubic spinel having $a = ca.$ 8.26 Å. As seen in Fig. 6, decomposition product of charged $LiCo_{1/3}Ni_{1/3}Mn_{1/3}O_2$ is identified as a cubic spinel. Although the ionic distribution of lithium and transition metals in a cubic close-packed oxygen array is not known yet, phase change from a layered to spinel-framework structure due to the mobile cation plays an important role on the suppression of active oxygen gas evolution by heating, as has been discussed by Delmas's research group [16,17] for lithium

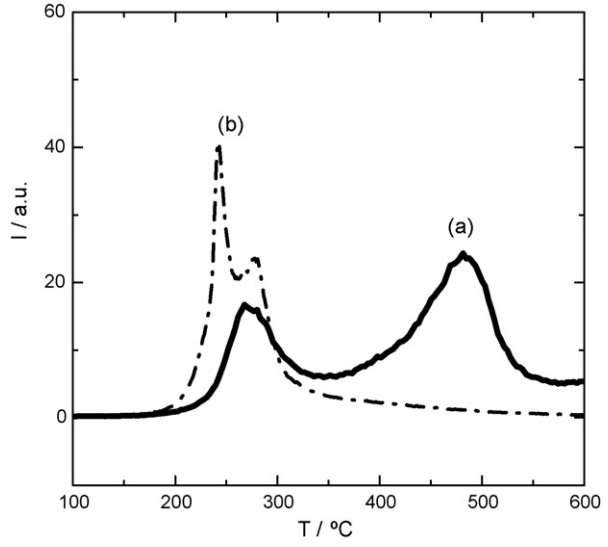

Fig. 5. The O_2-gas signals obtained by MS (31.7–32.7 in *m/z*) as a function of heating temperature for charged (a) $LiCo_{1/3}Ni_{1/3}Mn_{1/3}O_2$ (185 mAh g^{-1} of charge capacity) and (b) $LiCoO_2$ (140 mAh g^{-1} of charge capacity). The samples were electrochemically prepared without the addition of carbon and organic binders.

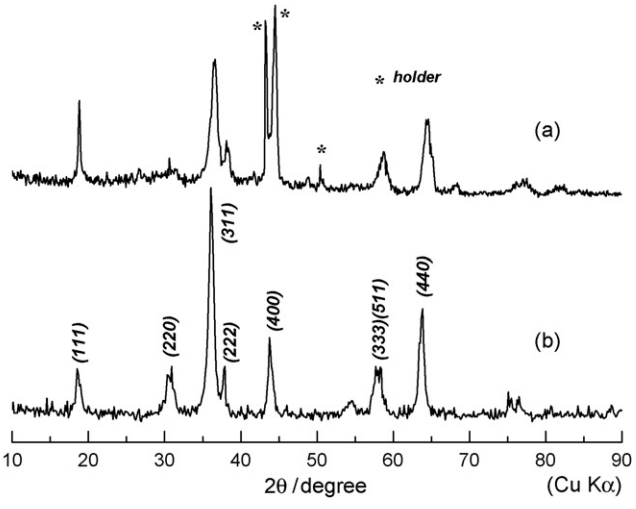

Fig. 6. High-temperature XRD pattern on (a) the decomposition products observed by heating the charged $LiCo_{1/3}Ni_{1/3}Mn_{1/3}O_2$ (charged at 4.45 V) at 400 °C. Decomposition product obtained by heating a precursor of cobalt nickel manganese hydroxide at 600 °C is also shown in (b). The precursor is used to prepare $LiCo_{1/3}Ni_{1/3}Mn_{1/3}O_2$. XRD pattern (b) is observed at room temperature.

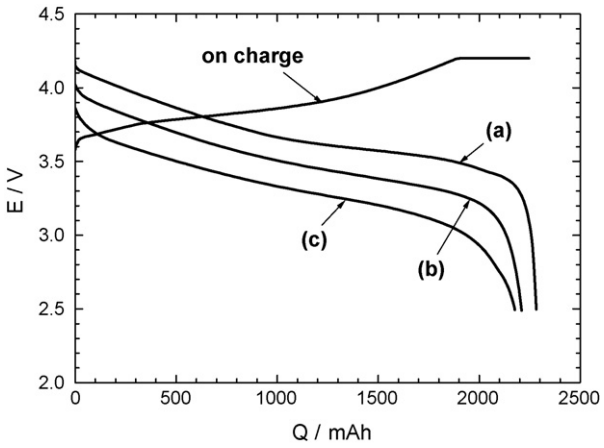

Fig. 7. Rate-capability tests on the lithium-ion battery (R18650; 2.3 Ah of nominal capacity) consisting of new positive electrode and graphite-negative electrode. The battery was discharged at (a) 430 mA, (b) 2150 mA, and (c) 4300 mA at 20 °C. The battery was charged at constant current of 1500 mA up to 4.2 V followed by charging at constant voltage of 4.2 V until charging current reaches below 110 mA.

nickel oxide derivatives. Mobile cations may be manganese ions because the thermal behaviors stated above are not observed for $LiCoO_2$ or more generally $LiCo_xNi_{1-x}O_2$ [18].

In order to bridge basic researches on lithium insertion materials and industrial technologies, basic research results on lithium cobalt nickel manganese oxide have been applied to the design for advanced lithium-ion batteries. After improving and adjusting several parametric factors to fabricate practical lithium-ion batteries, we have made lithium-ion batteries consisting of graphite and novel lithium insertion material. Fig. 7 shows the results of rate-capability tests on the cylindrical lithium-ion batteries R18650 having 2.3 Ah capacity, called CE2.3Ah in Fig. 1. The batteries are charged at constant current of 1500 mA to charge-end voltage of 4.2 V and then at constant voltage of 4.2 V until the current reaches below 110 mA at 20 °C, so-called CCCV. The batteries are discharged to 2.5 V at a rate of (a) 430 mA, (b) 2150 mA, and (c) 4300 mA at

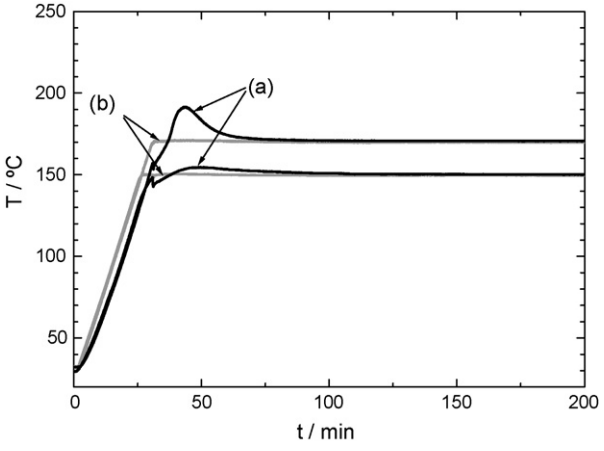

Fig. 8. Heating tests on the lithium-ion battery of new lithium insertion material and graphite (R18650-CE2.3Ah): (a) temperature on battery surface and (b) temperature in an oven. Heating rate is 5 °C min^{-1} up to 150 or 170 °C.

20 °C. As can be seen in Fig. 7, lithium-ion batteries show high rate discharge performance. Fig. 8 shows the results on heating tests of new R18650 lithium-ion batteries for high-power and high-energy density applications. After lithium-ion batteries were charged at CCCV of 1500 mA to 4.2 V, the batteries were heated up to 150 °C or 170 °C at a rate of 5 °C min^{-1} and kept at that temperature in an oven. The lithium-ion batteries do not show rapid increase in temperature associated with thermal runaway even when the batteries are heated at 170 °C [19].

4. Concluding remarks

In this paper, we have shown new lithium-ion batteries by applying novel lithium insertion material of lithium cobalt nickel manganese oxide. The batteries show high-power and high-energy densities with excellent cycle life and safety. Because thermal behaviors of the new batteries are much milder than that of current lithium-ion batteries of $LiCoO_2$, safety devices of PTC could be removed in designing lithium-ion batteries [20]. Actually, this type of new lithium-ion batteries for high-power application has been produced since late autumn in 2004, called CE2.3Ah in Fig. 1, and improved energy density in 2005, called DA2.5Ah showing more than 500 Wh dm^{-3} in energy density even for high-power applications. As were briefly described above, this type of lithium-ion battery is one of the promising lithium-ion batteries for high-power applications, such as hybrid electric vehicles and power tools.

Acknowledgement

The present work was partially supported by a grant-in-aid from the Osaka City University (OCU) Science Foundation.

References

[1] B. Ammundsen, J. Paulsen, Adv. Mater. 13 (2001) 943–956.
[2] M.S. Whittingham, Chem. Rev. 104 (2004) 4271–4301.
[3] T. Ohzuku, K. Ariyoshi, Y. Makimura, N. Yabuuchi, K. Sawai, Electrochemistry (Tokyo, Japan) 73 (2005) 2–11.
[4] H. Yoshizawa, M. Ikoma, J. Power Sources 146 (2005) 121–124.
[5] T. Ohzuku, Y. Makimura, Chem. Lett. 30 (2001) 642–643.
[6] T. Ohzuku, Y. Makimura, Chem. Lett. 30 (2001) 744–745.
[7] Y. Makimura, T. Ohzuku, J. Power Sources 119–121 (2003) 156–160.
[8] N. Yabuuchi, T. Ohzuku, J. Power Sources 119–121 (2003) 171–174.
[9] Y. Koyama, Y. Makimura, I. Tanaka, H. Adachi, T. Ohzuku, J. Electrochem. Soc. 151 (2004) A1499–A1506.
[10] Y. Koyama, N. Yabuuchi, I. Tanaka, H. Adachi, T. Ohzuku, J. Electrochem. Soc. 151 (2004) A1545–A1551.
[11] N. Yabuuchi, Y. Koyama, N. Nakayama, T. Ohzuku, J. Electrochem. Soc. 152 (2005) A1434–A1440.
[12] H. Yoshizawa, T. Ohzuku, Electrochemistry (Tokyo, Japan) 71 (2003) 1177–1181.
[13] H. Yoshizawa, T. Ohzuku, ITE Lett. 4 (2003) 569–572.
[14] J.R. Dahn, A.K. Sleigh, H. Shi, B.M. Way, W.J. Weydanz, J.N. Reimers, Q. Zhong, U. von Sacken, Lithium Batteries, in: G. Pistoia (Ed.), Industrial Chemistry Library, vol. 5, Elsevier, Amsterdam, 1994, pp. 1–47.
[15] J.R. Dahn, E.W. Fuller, M. Obrovac, U. von Sacken, Solid State Ionics 69 (1994) 265–270.

[16] M. Guilmard, L. Croguennec, D. Denux, C. Delmas, Chem. Mater. 15 (2003) 4476–4483.
[17] M. Guilmard, L. Croguennec, C. Delmas, Chem. Mater. 15 (2003) 4484–4493.
[18] H. Yoshizawa, T. Ohzuku, in abstract P-32 LiBD-3, Arcachon France, May 22–27, 2005.
[19] Data presented in Fig. 8 are for scientific description only, not intended to make or imply any guarantee or warranty.
[20] N. Yamamoto, H. Hiratsuka, S. Arimoto, H. Furuta, K. Kinoshita, Proceedings of the 22nd International Battery Seminar, Florida, March 15, 2005.